

# Processing and Characterization of a Polylactic Acid/Nanoclay Composite for Laser Sintering

Jiaming Bai,<sup>1</sup> Ruth D. Goodridge,<sup>2</sup> Richard J.M. Hague,<sup>2</sup> Masami Okamoto<sup>3</sup>

<sup>1</sup>3D Additive Manufacturing Group, Singapore Institute of Manufacturing Technology, 638075, Singapore

<sup>2</sup>Additive Manufacturing and 3D-Printing Research Group, Faculty of Engineering, University of Nottingham, NG7 2RD, UK

<sup>3</sup>Polymeric Nanocomposites Laboratory, Toyota Technological Institute, Nagoya 468-8511, Japan

**In this work, the feasibility of processing polylactic acid (PLA) and a PLA/nanoclay composite by laser sintering (LS) were investigated. The morphology of both the PLA and PLA/nanoclay powder was examined by scanning electron microscopy. LS process parameters, especially powder bed temperature, laser power, and laser scan count were studied. The effect of the addition of nanoclay on the thermal and flexural properties of LS PLA parts was examined. The results showed that PLA/nanoclay required a lower processing powder bed temperature compared with neat PLA. Under the same powder bed temperature, PLA/nanoclay parts exhibited an improvement in flexural modulus compared with neat PLA. Flexural modulus was increased significantly with double scan for both neat PLA and PLA/nanoclay LS parts. POLYM. COMPOS., 00:000–000, 2015. © 2015 Society of Plastics Engineers**

## INTRODUCTION

Additive Manufacturing (AM), which is an outgrowth of rapid prototyping, aims to offer greater flexibility in respect to product design and manufacture compared with traditional manufacturing routes. Previously referred to as Rapid Manufacturing, AM is defined as “the use of a computer aided design (CAD)-based automated AM process to construct parts that are used directly as finished products or components” [1].

The capabilities of AM have resulted in numerous changes to the traditional product design and manufacturing process. With additive techniques not using mold tooling and being cost-effective for low volume parts, it is feasible to introduce new products in low quantities to see whether a market demand exists for them. In addition,

when highly complex components are produced without any need for tools or a mold, the lead-time and the overall manufacturing costs for items will be reduced [2]. AM can also reduce the need for assembly processes by building a multi-component unit as a singular unit, without any fastening mechanism. Furthermore, customer input and customisation are also benefits of design for AM [3].

One of the most widely used AM techniques, laser sintering (LS), also referred to as Selective Laser Sintering (SLS<sup>TM</sup>), is a powder-based additive-layer manufacturing process. In the LS process a laser, either in continuous or pulse mode, is used as a heat source for scanning and joining powder particles into predetermined shapes. The geometry of the scanned layers corresponds to the various cross sections of the CAD model and STL file of the object.

Thermoplastic materials are well-suited for powder bed processing because of their relatively low melting temperature and low thermal conductivities [4]. Polyamide 12 (PA12), which is the most common LS material, has been developed and used to create functional parts. However, limitations exist with current LS materials. Firstly, due to complex thermal phenomena during the LS process, there is a very limited choice of polymers which are able in practice to be processed at present [5]. Secondly, the polymers that are available for LS cannot completely meet the needs, such as the mechanical requirements, of all products. To further develop AM, there is a growing need to research and develop more materials which can meet the various requirements for different applications.

Polylactic acid (PLA), which is a thermoplastic, compostable, biodegradable and biocompatible polymer, is attracting much interest as it is derived from renewable resources and has a number of promising applications, especially in the biomedical field [6, 7]. The US Food and Drug Administration approved PLA for the construction of tissue engineering (TE) scaffolds [8]. Some attempts

Correspondence to: Jiaming Bai; e-mail: baijm@simtech.a-star.edu.sg  
DOI 10.1002/pc.23848

Published online in Wiley Online Library (wileyonlinelibrary.com).

© 2015 Society of Plastics Engineers

have been made to process PLA for medical applications using AM, for example, Patricio et al. [9] fabricated a PLA/PCL scaffolds for tissue engineering with a biomanufacturing device, which showed improved biological and mechanical properties.

One shortcoming for PLA is that, compared to metal and ceramics, its strength and stiffness are very low [10]. To improve the strength and stiffness, inorganic fillers have been used to form PLA-filler composites. A filler, typically micron-sized, is added into the polymer matrix to improve its properties. In a polymer-filler composite system, chemical bonding is rarely involved, and the polymer matrix and the fillers are connected to each other by weak intermolecular forces. If the filler is in the nanoscale, the reinforcing material in the composite can be dispersed on a molecular scale (nanometre level) and interacts with the polymer matrix by chemical bonding. If this can be achieved, significant improvements in the mechanical properties or thermal properties of the material might be obtained [11]. Iturrondobetia et al [12] studied the thermal influence of nanoclay on PLA/nanoclay nanocomposites. It was found that nanoclays can improve the thermal stability of PLA by increasing the degradation temperature and decreasing the degradation rate. Gloria et al. [13] reviewed the application of fibre-reinforced composite materials in the aerospace, aeronautical, and biomedical areas.

Nanofiller-reinforced polymers offer the potential to improve the base material's properties while remaining processible by conventional processing techniques and this potential is also expected for the LS process. Several attempts have been made to improve the mechanical or physical properties of matrix polymers used for LS by adding a nanofiller [14–16]. In our previous study, PA12-Carbon nanotube (CNT) nanocomposite powder was produced with spherical morphology and suitable particle size for processing by LS. Compared with the laser-sintered PA12 parts, PA12-CNT parts showed significantly enhanced mechanical properties, which may be attributed, to the good dispersion of the CNT in the PA12 matrix and denser laser-sintered parts [16, 17].

LS has previously been used to design and produce PLA scaffolds with highly complex porous networks in a limited number of studies. Tan et al. [18] applied the LS technique to fabricate PLA scaffold specimens, which were examined using a Scanning Electron Microscope (SEM), but without measuring the material or mechanical properties. Zhou et al. [19] successfully fabricated a porous bone TE scaffold with Poly(L-lactide) (PLLA), which is a form of PLA, and PLLA/carbonated hydroxyapatite nanocomposite via LS. However, the effect of a nanofiller on the processing and mechanical properties of PLA LS samples was not studied.

In this work, the feasibility of processing PLA and a PLA/nanoclay composite by LS was investigated. The LS process parameters for PLA/nanoclay composite, as well as for neat PLA, were studied. The effect of the addition of nanoclay on the processing and mechanical properties of LS PLA parts was also examined.

## EXPERIMENTAL

### *Materials*

PLA was obtained from Toyota Technological Institute, Japan. The PLA had a D content of 1.1–1.7%. The nanoclay filler used in this study was organically modified montmorillonite, which was supplied by Nanocor, Japan. The PLA/nanoclay composite was prepared by melt mixing and extrusion at 190°C to yield nanocomposite strands. According to the literature, the typical nanoclay loading for the nanocomposite is from 0.5 to 10 wt% to secure mechanical property improvements [12]. In this study, 5 wt% nanoclay, which is an intermediate value, was chosen to produce the PLA/nanoclay composite. Both the PLA and PLA/nanoclay powders were cryogenically fractured, with an average particle size of 30 µm, for LS.

### *Laser Sintering*

The neat PLA and PLA/nanoclay composite materials were LS on an EOS P100 Formiga system. The powders were dried in an oven at 40°C for 8 h before LS. Both powders spread relatively well during the process; however, they were attracted to the metal surfaces of the machine. To determine the optimum processing parameters in terms of ease of processing and achieving the highest mechanical properties, different processing parameters, including powder bed temperature, laser power, and laser scan count were investigated.

Flexural test specimens of both PLA and PLA/nanoclay were built to establish the mechanical properties according to ASTM D790. The flexural test specimens were arranged with the longest dimension arranged vertically to the direction of movement of the recoating blade.

### *Characterization*

The morphologies of the neat PLA and PLA/nanoclay composite powders were imaged using a LEO 440 SEM (Leo Electron Microscopy Ltd). The powders were coated with gold before SEM characterisation to prevent charging. SEM was also used to analyse the morphology of a cross section of the flexural testing bars and the degree of sintering. The flexural properties were measured on a Zwick 103 (Zwick/Roell Corporation) testing machine using a 3-point bending test method at a test speed of 5 mm/min, following ASTM D790. Five samples were tested each time to obtain average values (Figure 1). The thermal behavior of both neat PLA and PLA/nanoclay powders was studied by differential scanning calorimetry (DSC) using a SHIMADZU DSC-60 instrument. Samples weighing 5 mg were heated at 20°C/min to obtain the melting curves, from which melting temperature ( $T_m$ ) and glass transition temperature ( $T_g$ ) were determined for each powder. The thermal properties of LS neat PLA and PLA/nanoclay composite parts were also examined by DSC using identical parameters.

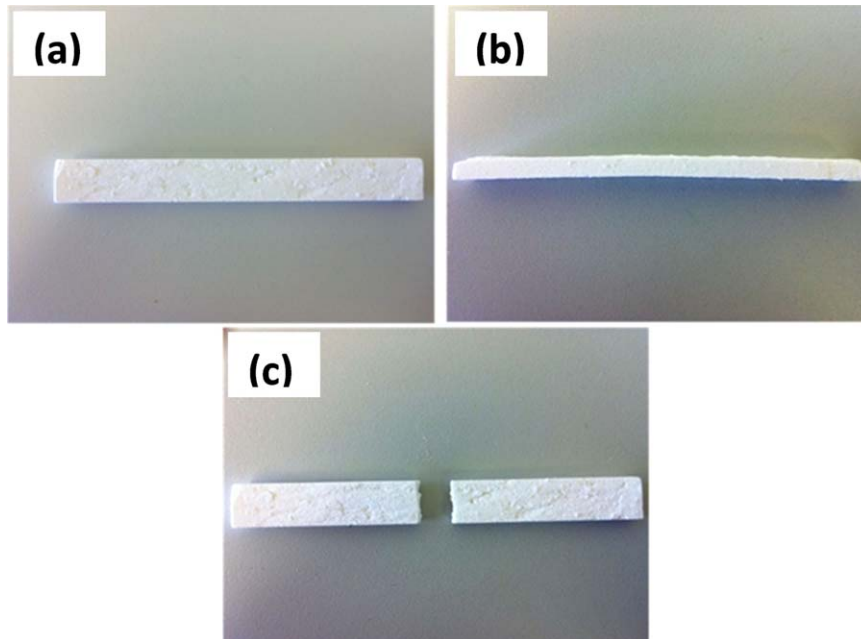


FIG. 1. Flexural test parts (a) top-view, (b) side-view, and (c) tested part. [Color figure can be viewed in the online issue, which is available at [wileyonlinelibrary.com](http://wileyonlinelibrary.com).]

## RESULTS AND DISCUSSION

### *Powder Morphology*

The PLA and PLA/nanoclay composite powders were relatively easy to spread over the build area of the LS machine at room temperature. However, compared to commercial polyamide 12 (PA12) LS materials, both neat PLA and PLA/nanoclay composite powders exhibited inferior flowability, having increased tendency to agglomerate and adhere to metallic surfaces. This may be due to their small particle size of  $30\ \mu\text{m}$ , which is smaller than the normally recommended powder particle size  $45\text{--}90\ \mu\text{m}$  for LS [20]. Compared with large particles, small particles are easier to agglomerate during the LS process [5].

Figure 2 shows the SEM micrographs for the neat PLA and PLA/nanoclay composite powders. No obvious difference in the powder surface morphology between the neat PLA and the PLA/nanoclay composite powders could be seen. However, both powders had irregular, angular, and porous particles. Irregular and nonuniform powder morphology is known to have a negative effect on the powder flowability, as well as the density of the sintered parts and the mechanical properties of LS parts [21]. Powders with regular morphologies tend to arrange themselves more efficiently, which increases the density of parts, while particles with irregular morphologies are not able to achieve this form of efficient arrangement resulting in low density parts. Therefore, spherical particles are usually preferred for LS. As the powder particles are not fully melted in the LS process, the pores existing in individual particles may

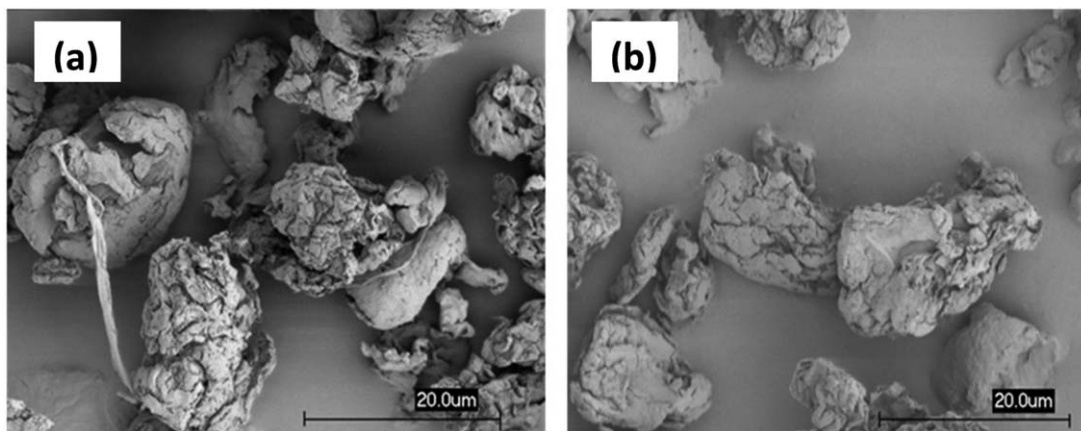


FIG. 2. SEM micrographs of (a) neat PLA powder and (b) PLA/nanoclay composite powder.

remain in the LS parts, and thus nonporous particles are evidently favored [21].

### Powder Bed Temperature

During the LS process, the powder bed temperature is normally controlled to prevent distortion of the parts, mainly “curling,” or “caking” of the powder bed. The powder bed should be kept uniform and agglomerate-free to achieve repeatable results. Curling occurs when the powder bed temperature is too low, which causes a high thermal gradient between the sintered and unsintered material. When the powder bed temperature is too high, “caking” is observed; a phenomenon whereby the powder particle surface starts to melt and powder sticks together, which leads to powder agglomeration [5].

Theoretically, the powder bed temperature should be kept as high as possible but below the melting temperature ( $T_m$ ) for semicrystalline polymers, or glass transition temperature ( $T_g$ ) for amorphous polymers, to achieve optimum mechanical properties with relatively low laser input. For example, the powder bed temperature for the most commonly used commercial LS material, PA12, which is a semicrystalline polymer with  $T_g$  at 40°C – 50°C and melting point around 180°C, was set close to its  $T_m$ , at about 170°C [22]. However, in practice, choosing the correct powder bed temperature for LS is highly dependent on the choice of material. The required powder bed temperature is material specific and needs to be determined in practice for new materials.

PLA, used in this study, is a semicrystalline material, and the  $T_g$  and  $T_m$  for PLA and the PLA/nanoclay are shown in Table 1. To determine the optimum powder bed temperature, the temperature was initially set at 40°C and increased by 10°C increments until the powder cake became too hard or agglomerates were found. Then, the temperature was reduced by 2°C each time until free powder flow and a smooth powder bed without caking

TABLE 1. Thermal temperature obtained from the DSC curves of PLA/nanoclay and PLA powders.

Material	Powder Bed Temperature (°C)	Laser power (W)	Laser scan count
Neat PLA	60	15	Single
	60	16	Single
	60	17	Single
	60	17	Double
	70	16	Single
	80	16	Single
	80	17	Single
PLA/nanoclay	60	15	Single
	60	16	Single
	60	17	Single
	60	17	Double

LS parameters for neat PLA and PLA/nanoclay composite (laser scan speed = 2500 mm/s, scan spacing = 0.25 mm).

TABLE 2. Thermal temperatures obtained from the DSC curves of PLA/nanoclay and PLA powders.

Samples	$T_g$ (°C)	$T_{om}$ (°C)
PLA/nanoclay	65.3	144.7
PLA	71.8	146.5

LS parameters for neat PLA and PLA/nanoclay composite (Laser scan speed = 2500 mm/s, scan spacing = 0.25 mm).

was obtained. By this method, the suitable powder bed temperature for neat PLA powder was found to be 80°C. In the case of PLA/nanoclay, the powder bed temperature was found to be 60°C, which was noticeably lower than the neat PLA powder.

To compare the neat PLA and PLA/nanoclay composite LS parts in parallel, 60°C was selected as the powder bed temperature during LS for both materials. At the same time, neat PLA was also LS at powder bed temperatures of 70 and 80°C, to investigate the effect of powder bed temperature on the mechanical properties of LS parts. The LS process conditions for each powder, with which flexural test specimens were built successfully, are shown in Table 2. The laser power and laser scan count will be discussed in later sections.

### Thermal Analysis of PLA and PLA/Nanoclay Powders and LS Parts

The DSC curves for the PLA and PLA/nanoclay composite, both in powder and sintered part form, are shown in Figure 3. The glass transition temperature  $T_g$  and onset melting temperature  $T_{om}$  for neat PLA and PLA/nanoclay composite powders were obtained, shown in Table 1. It can be seen that the  $T_g$  and  $T_{om}$  of PLA/nanoclay were 6.5 and 1.8°C lower than those of neat PLA. By adding nanoclay into PLA, both  $T_g$  and  $T_{om}$  decreased. This might be one reason that the processing powder bed temperature of PLA/nanoclay was lower than the neat PLA.

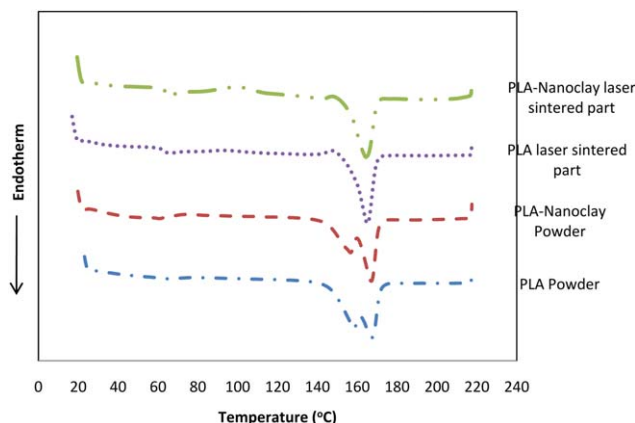


FIG. 3. DSC curves of PLA and PLA/nanoclay composite powders and LS parts. [Color figure can be viewed in the online issue, which is available at [wileyonlinelibrary.com](http://wileyonlinelibrary.com).]

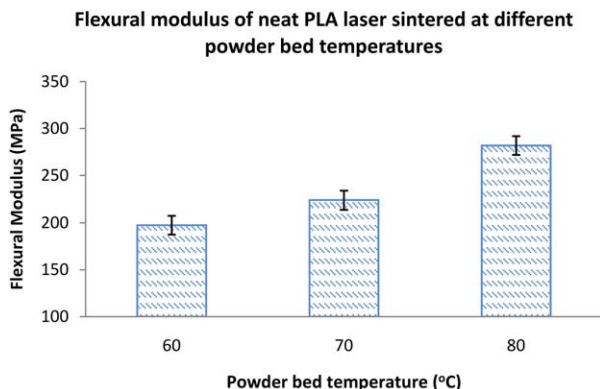


FIG. 4. Variation in flexural modulus with respect to powder bed temperature (Laser power = 16 W, Laser scan speed = 2500 mm/s, scan spacing = 0.25 mm, single scan). [Color figure can be viewed in the online issue, which is available at wileyonlinelibrary.com.]

The DSC curves also showed that there were two melting peaks in both PLA and PLA/nanoclay powders. The double melting behavior in PLA has previously been explained as being due to the increase in crystallinity through melt recrystallization [23]. The lower-temperature peak corresponds to the melting of a small amount of the original crystals, and the higher-temperature peak is attributed to the melting of crystals formed through a melt-recrystallization process during a heating scan. The recrystallization in the process causes the exothermic peak between the double melting peaks. After LS, there was only one melting peak remaining for both PLA and PLA/nanoclay LS parts, which indicates that the crystallites formed in the melt-crystallized process during LS process is unimodal (single crystallite structure). The disappearance of another peak was due to the melting and recrystallization occurring simultaneously [24, 25].

#### Mechanical Characterization of LS Parts

**Dependence of Flexural Modulus on Powder Bed Temperature.** The effect of powder bed temperature on flexural modulus was investigated. Figure 4 shows the

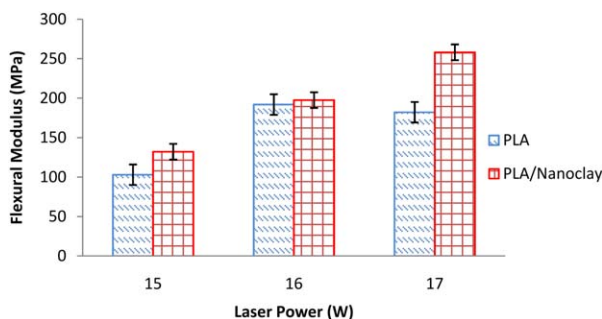


FIG. 5. Variation in flexural modulus with respect to laser power for PLA and PLA/nanoclay (powder bed temperature 60 °C). [Color figure can be viewed in the online issue, which is available at wileyonlinelibrary.com.]

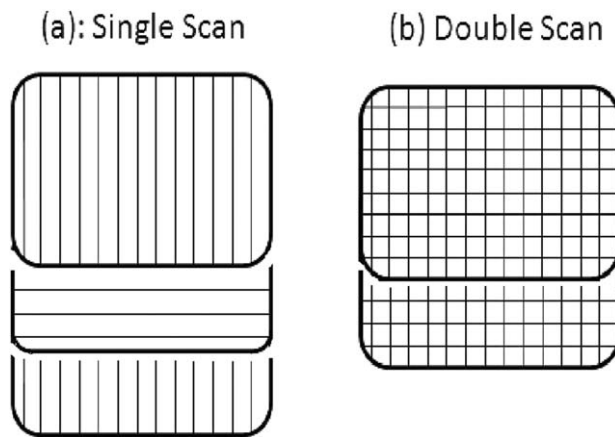


FIG. 6. Schematic of single laser scan and double laser scan.

flexural modulus of neat PLA LS parts at different powder bed temperatures with constant laser power. It can be seen that as the powder bed temperature was increased from 60 to 80 °C, the flexural modulus of the produced parts also increased. This indicated that at the same laser scan conditions (laser power, scan speed, and scan type), parts built with a higher powder bed temperature had better mechanical properties. This increase in mechanical properties with bed temperature is typical for LS polymers [26].

**Dependence of Flexural Modulus on Laser Power and Nanofiller.** The dependence of laser power on flexural modulus for the LS PLA and PLA/nanoclay composite parts is shown in Figure 5. Flexural parts were built using three different laser powers: 15, 16, and 17 W, keeping the powder bed temperature constant at 60 °C. As expected, parts made with a higher laser power showed an improvement in flexural modulus for both neat PLA and PLA/nanoclay. Compared to neat PLA processed under these conditions, PLA/nanoclay parts exhibited an improvement of between 3.1 and 41.5% in flexural modulus.

However, it is noticeable that the neat PLA part LS at a powder bed temperature of 80 °C showed a higher flexural modulus (304.3 MPa) than that of PLA/nanoclay part (258.2 MPa) LS at a powder bed temperature of 60 °C with a same laser power of 17 W. As the PLA/nanoclay cannot be processed above 60 °C due to powder agglomeration, no direct comparison was possible in this case.

**Dependence of Flexural Modulus on Laser Scan Count.** In this study, two kinds of laser scan were applied for LS: single laser scan and double laser scan. In single scan, the laser scans each layer once before recoating, whilst with double scan, each layer is scanned twice. In single scan, alternate layers are scanned in the vertical and horizontal directions. In double scan, each layer is scanned in both the vertical and horizontal directions before recoating, shown in Figure 6. Double scan can deliver the laser energy to each layer in a more gradual manner, resulting in

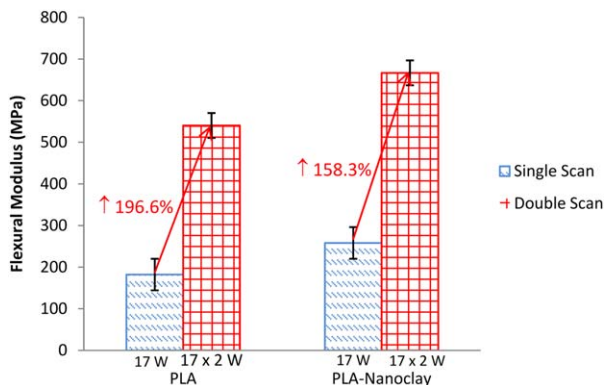


FIG. 7. Variation in flexural modulus with respect to laser scan type for PLA and PLA/nanoclay. [Color figure can be viewed in the online issue, which is available at [wileyonlinelibrary.com](http://wileyonlinelibrary.com).]

the release of structural stresses in sintered parts, which results in less shrinkage and curling [27].

In a laser energy input range where the polymer does not degrade, higher laser energy input can lead to improved mechanical properties of sintered parts. In the actual experimental process of this work, laser scan count started with a single scan. It was found that the highest laser power that could be inputted was 17 W for single scan. Parts started to curl and the build failed if the laser power exceeded 17 W. A double laser scan was performed to improve the laser energy input without parts curling. In the work carried out by Goodridge et al. [27], when applying double scan on target parts, the laser power was reduced to avoid over energy input, thus preventing shrinkage and curling. In this work, when applying double scan on the neat PLA and PLA/nanoclay composite powders, it was found that the laser power could be inputted as high as the highest single scan count power, which was 17W. With 17 W laser power, there was no obvious increase in curling of the sintered parts when double scan was applied for both PLA and PLA/nanoclay powders. Curling appeared when the double scan laser power was higher than 17 W, which was same as single scan.

Figure 7 records the variation in flexural modulus with respect to laser scan count. It can be seen that compared with single scanned parts, the flexural modulus for parts built by double scan had more than 100% percent increase (196.6% for PLA, 158.3% for PLA/nanoclay). This significant rise in flexural modulus suggested that double scan is a possible way to further mechanical properties of LS PLA and PLA/nanoclay. However, the processing time for double scan is longer compared with single scan, which increases the whole processing period.

#### Characterization of LS Parts

Figure 8 shows SEM micrographs of the cross sectional surfaces of LS neat PLA and PLA/nanoclay composite parts. The sintered and unsintered powder, as well as the layer and porous structure can be seen from the LS parts, which indicated that not all powders were fully melted during the LS process for both PLA and PLA/nanoclay. Porosity has been found to have a major influence on the mechanical properties of LS parts, in order of decreasing severity: fracture, fatigue, strength, ductility, and modulus [1]. The pores in the sintered parts, as well as the pores in the individual unsintered powder were contributing to the relatively low mechanical properties of LS parts. Further investigation is needed to reduce the porosity of PLA/PLA/nanoclay materials, which will lead to improvements in their mechanical properties.

#### CONCLUSIONS

A study was performed to explore the feasibility of using LS to process neat PLA and PLA/nanoclay composite. It has been demonstrated that:

- It was possible to LS nanoclay reinforced PLA to achieve well defined parts, such as flexural test specimens, with precise LS parameters.
- Under the same processing parameters, the PLA/nanoclay LS samples showed an increased flexural modulus compared to the neat PLA samples produced. However, neat

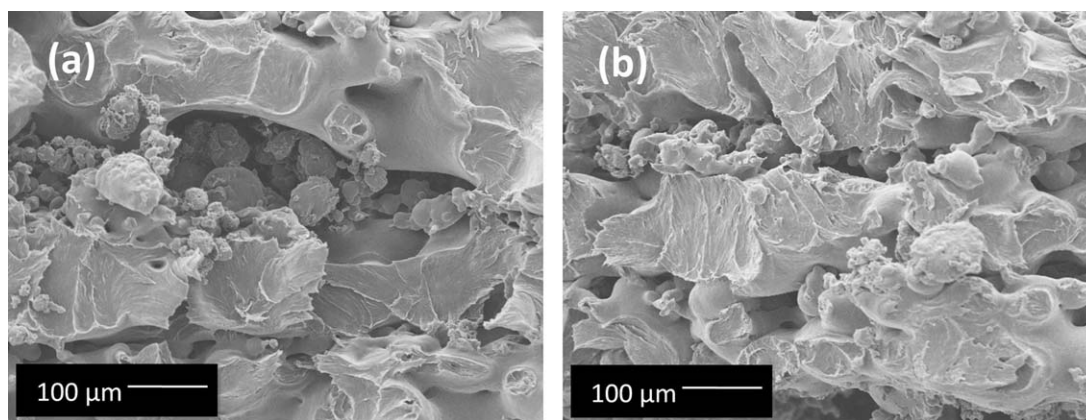


FIG. 8. SEM images of cross section of LS (a) PLA, and (b) PLA/nanoclay.

PLA had higher powder bed processing temperature compared to PLA/nanoclay, which ultimately led to higher flexural properties.

- Compared with single laser scan, double scan lead to a significant increase in flexural modulus for both neat PLA and PLA/nanoclay. Besides considering parameters such as powder bed temperature, laser power, laser scan spacing, and scan speed, the scan count should also be considered as a way to increase energy input gradually and improve parts' mechanical properties.

## REFERENCES

1. N. Hopkinson, R.J.M. Hague, and P.M. Dickens, *Rapid Manufacturing: An Industrial Revolution for the Digital Age*, John Wiley, England (2006).
2. R. Hague\*, S. Mansour, and N. Saleh, *Int. J. Production Res.*, **42**, 4691 (2004).
3. R. Hague, I. Campbell, and P. Dickens, *Proc. IME. C-J. Mech. Eng.*, **217**, 25 (2003).
4. J.P. Kruth, G. Levy, F. Klocke, and T.H.C. Childs, *CIRP Ann.-Manufacturing Technol.*, **56**, 730 (2007).
5. R.D. Goodridge, C.J. Tuck, and R.J.M. Hague, *Prog. Mater. Sci.*, **57**, 229 (2012).
6. J. Lunt, *Polym. Degrad. Stab.*, **59**, 145 (1998).
7. B. Conti, F. Pavanetto, and I. Genta, *J. Microencapsul.*, **9**, 153 (1992).
8. M. Wang, *Am. J. Biochem. Biotechnol.*, **2**, 80 (2006).
9. T. Patrício, M. Domingos, A. Gloria, U. D'Amora, J.F. Coelho, and P.J. Bártolo, *Rapid. Prototyping. J.*, **20**, 145 (2014).
10. S.S. Kim, M. Sun Park, O. Jeon, C. Yong Choi, and B.S. Kim, *Biomaterials*, **27**, 1399 (2006).
11. Y.W. Mai, Z.Z. Yu, *Polymer Nanocomposites*, Elsevier Science, 2006.
12. M. Iturrondobeitia, A. Okariz, T. Guraya, A.M. Zaldua, and J. Ibarretxe, *J. Appl. Polym. Sci.*, **131**, (2014). n/a-n/a.
13. A. Gloria, D. Ronca, T. Russo, U. D'Amora, M. Chierchia, R. De Santis, L. Nicolais, and L. Ambrosio, *J. Appl. Biomech. Biomech.: JABB*, **9**, 151 (2011).
14. H. Chung and S. Das, *Mater. Sci. Eng. A*, **487**, 251 (2008).
15. J. Bai, R.D. Goodridge, R.J.M. Hague, M. Song, and M. Okamoto, *Polym. Test.*, **36**, 95 (2014).
16. J. Bai, R.D. Goodridge, R.J.M. Hague, and M. Song, *Polym. Eng. Sci.*, **53**, 1937 (2013).
17. J. Bai, R.D. Goodridge, R.J.M. Hague, M. Song, and H. Murakami, *J. Mater. Res.*, **29**, 1817 (2014).
18. K.H. Tan, C.K. Chua, K.F. Leong, C.M. Cheah, W.S. Gui, W.S. Tan, and F.E. Wiria, *Biomed. Mater. Eng.*, **15**, 113 (2005).
19. W. Zhou, S. Lee, M. Wang, W. Cheung, and W. Ip, *J. Mater. Sci.: Mater. Med.*, **19**, 2535 (2008).
20. R.D. Goodridge, K.W. Dalgarno, and D.J. Wood, *Mech. Eng. H.*, **220**, 57 (2006).
21. N. Karapatis, G. Egger, P. Gygax, and R. Glardon, Optimization of powder layer density in selective laser sintering, International solid freeform fabrication symposium - An additive manufacturing conference Austin, TX, 1999.
22. R.D. Goodridge, M.L. Shofner, R.J.M. Hague, M. McClelland, M.R. Schlea, R.B. Johnson, and C.J. Tuck, *Polym. Test.*, **30**, 94 (2011).
23. M. Yasuniwa, S. Tsubakihara, K. Iura, Y. Ono, Y. Dan, and K. Takahashi, *Polymer*, **47**, 7554 (2006).
24. M. Yasuniwa, S. Tsubakihara, Y. Sugimoto, and C. Nakafuku, *J. Polym. Sci. Part B: Polym. Phys.*, **42**, 25 (2004).
25. M. Yasuniwa, K. Sakamo, Y. Ono, and W. Kawahara, *Polymer*, **49**, 1943 (2008).
26. B. Caulfield, P.E. McHugh, and S. Lohfeld, *J. Mater. Process. Technol.*, **182**, 477 (2007).
27. R.D. Goodridge, R.J.M. Hague, and C.J. Tuck, *J. Mater. Process. Technol.*, **210**, 72 (2010).